CO + H SUB 2 REACTION OVER NITROGEN-MODIFIED IRON CATALYSTS. QUARTERLY TECHNICAL PROGRESS REPORT, JULY 1-SEPTEMBER 30, 1984

PURDUE UNIV.
LAFAYETTE, IN

JAN 1985

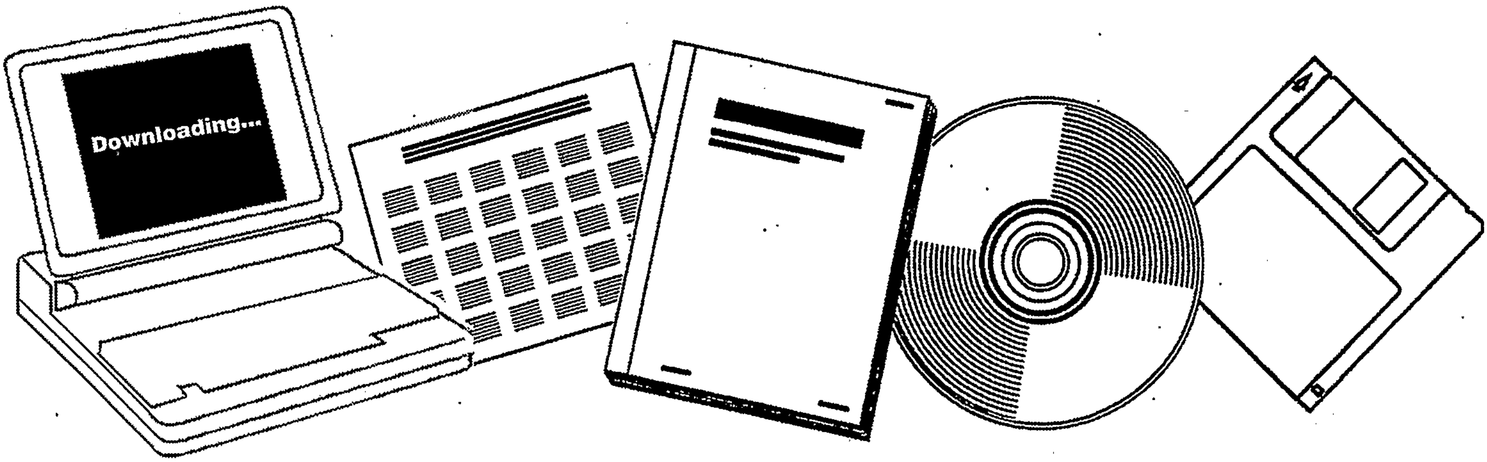

One Source. One Search. One Solution.

NTIS

Providing Permanent, Easy Access to U.S. Government Information

National Technical Information Service is the nation's largest repository and disseminator of government-initiated scientific, technical, engineering, and related business information. The NTIS collection includes almost 3,000,000 information products in a variety of formats: electronic download, online access, CD-ROM, magnetic tape, diskette, multimedia, microfiche and paper.

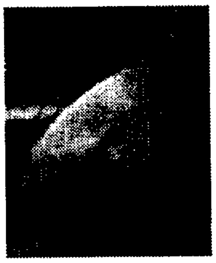

Search the NTIS Database from 1990 forward

NTIS has upgraded its bibliographic database system and has made all entries since 1990 searchable on **www.ntis.gov.** You now have access to information on more than 600,000 government research information products from this web site.

Link to Full Text Documents at Government Web Sites

Because many Government agencies have their most recent reports available on their own web site, we have added links directly to these reports. When available, you will see a link on the right side of the bibliographic screen.

Download Publications (1997 - Present)

NTIS can now provides the full text of reports as downloadable PDF files. This means that when an agency stops maintaining a report on the web, NTIS will offer a downloadable version. There is a nominal fee for each download for most publications.

For more information visit our website:

www.ntis.gov

U.S. DEPARTMENT OF COMMERCE
Technology Administration
National Technical Information Service
Springfield, VA 22161

DE85004875

DOE/PC/50804-8
(DE85004875)
Distribution Category UC-90a

DOE/PC/50804-8

CO + H_2 Reaction Over Nitrogen-Modified Iron Catalysts

Quarterly Technical Progress Report
for the Period July 1, 1984 - Sept. 30, 1984

W. Nicholas Delgass
Purdue University
West Lafayette, Indiana 47907

PREPARED FOR THE
U.S. DEPARTMENT OF ENERGY

Page Intentionally Left Blank

TABLE OF CONTENTS

Page

TABLE OF CONTENTS iii

LIST OF FIGURES v

LIST OF TABLES iv

ABSTRACT 1

1. OBJECTIVE AND SCOPE 2
   1.1 Background 2
   1.2 Objectives 3

2. TECHNICAL PROGRESS 4
   2.1 Summary of Results 4
   2.2 Mössbauer Spectroscopy 6
   2.3 Transient Kinetics 41

3. FUTURE RESEARCH 46

4. REFERENCES 46

List of Figures

		Page
Figure 1	Mössbauer Spectra of Single Phase Nitrides.	7
Figure 2	Mössbauer Spectra of γ'–Fe_4N.	12
Figure 3	Mössbauer Spectra of ϵ–Fe_xN.	14
Figure 4	Variation in Magnetic Splitting with ϵ–Nitride Composition.	18
Figure 5	Mössbauer Spectra of ζ–Fe_2N.	19
Figure 6	*In Situ* Analysis of ζ–Fe_2N Stability at 523 K.	21
Figure 7	*In Situ* Analysis of ζ–Fe_2N Dentriding.	23
Figure 8	Mössbauer Spectra of Partly Denitrided ζ–Fe_2N.	24
Figure 9	Mössbauer Spectra of Partly Denitrided ζ–Fe_2N Intermediate.	29
Figure 10	Mössbauer Spectra of Partly Nitrided α–Fe.	31
Figure 11	*In Situ* Analysis of α–FeNitriding.	33
Figure 12	Mössbauer Spectra of He Treated Nitrides.	37
Figure 13	Transient Response of ζ–Fe_2N to a 1 minute pulse of CO followed by a step to $3H_2/CO$ synthesis gas at 523 K.	42

List of Tables

Page

Table 1 Mössbauer Parameters (298 K) of Single Phase Nitrides 8

Table 2 Mössbauer Parameters of Non-equilibrium Nitrides. 27

Table 3 Mössbauer Parameters (298 K) of He Treated Nitrides. 39

Page Intentionally Left Blank

ABSTRACT

Detailed curve-fitting of the Mössbauer spectra of the pure nitrides has produced a quantitative description of the spectral components and of the structural features of the pure nitrides. This information has then been used to quantitatively follow loss of nitrogen from ζ-Fe_2N in H_2 and in He. A shrinking core model accounts for N loss in H_2 at 473K. N loss in He is not great at temperatures below 600K. Transient kinetics studies by mass spectrometry show that precarburizing Fe_2N with CO moderates nitrogen loss, but after an induction period NH_3 production leads CH_4 production. Thus, surface N loss is not effectively prevented by this pretreatment.

1. OBJECTIVES AND SCOPE

1.1 BACKGROUND

The feasibility of utilizing synthesis gas (CO + H_2) via the Fischer-Tropsch reaction pathway for the production of fuels and chemicals is well established. The SASOL ventures, for example, take advantage of abundant coal resources to produce both desirable synthetic automotive fuels and basic chemical feedstocks. The applicability of these chemical transformations is nonetheless limited. The present procedure requires extensive processing if the production of non-essential byproducts is to be avoided. The discovery and subsequent usage of improved catalysts would therefore be advantageous.

Experimental results published in the current literature show that nitrogen affects the performance of iron catalysts-catalysts which find widespread use in the Fischer-Tropsch synthesis route. Prenitriding of the iron catalyst has been reported to shift the product distribution to one exhibiting lower molecular weight fractions and enhanced alcohol yields (7). On the other hand, simultaneous introduction of ammonia (NH_3) with synthesis gas produces nitrogeneous compounds. Furthermore, and probably of greater importance, this addition of ammonia effects a reduction in the overall chain length of compounds in the product spectrum. It is of considerable interest, therefore, to study these and other characteristics of nitrided iron catalysts in order to gain a basic understanding of their behavior. Discovery of the new pathways in Fischer-Tropsch synthesis afforded by nitrogen will add to the fundamental knowledge from which future synthesis-catalysts can be derived.

1.2 OBJECTIVES

The scope of the program may be broken down into two main areas of concern. Firstly, consideration must be given to the role of the surface nitrogen in

i. altering the product distribution and

ii. stabilizing catalyst activity

of the synthesis reactions. *In-situ* Mössbauer studies identify the various iron nitride phases and allow for examination of their stability during reaction. The Mössbauer results form the basis for detailed kinetic tracer experiments involving transient and isotope labeling analyses. Ultrahigh vacuum work using SIMS and AES will supplement the Mössbauer and kinetic characterizations.

The second area of consideration will involve the kinetic and catalytic effects observed during the addition of ammonia to the synthesis gas stream. Transient work will be ideal for observing initial activity changes occurring as a result of NH_3 pulses. Along with ultrahigh vacuum studies, the transient kinetics of NH_3 addition will help clarify which steady state experiments would be most productive. The various analytical methods will define interactions between surface and bulk nitrogen, and their role in effecting new reaction pathways.

The primary experiments which define our route to understanding which parameters influence the selectivity and alter the activity of synthesis reactions may, therefore, be outlined as follows:

i. Mössbauer and simultaneous kinetics of prenitrided iron catalysts will be used to determine nitride phase stability and to correlate these phases to reaction selectivity. The initial pressure of one atmosphere may later be increased.

ii. Similar analysis of the effects of addition of NH_3 to the reactant stream will be performed.

iii. Transient analysis and isotope tracer studies of synthesis reactions over prenitrided catalysts will determine surface nitride stability. The stoichiometry at the surface and influence of nitriding on CO dissociation will be sought.

iv. Ultrahigh vacuum analysis will examine surface stoichiometry and reaction intermediates. Interaction between the nitrided phases and adsorption bond strengths of CO and H_2 will be investigated.

v. The effects of NH_3 addition to the reactant stream will be similarly followed by UHV and transient tracer studies to determine possible alterations in reaction pathways invoked by the presence of NH_3.

Computer modeling will be undertaken to aid in quantitative interpretation of transient data.

2. TECHNICAL PROGRESS

2.1 Summary of Results

A qualitative description of *in-situ* nitride decomposition during reaction has been previously considered using the powerful technique of Mössbauer spectroscopy. In this report, we have curve-fit the Mössbauer parameters for each of the nitrides in order to quantitatively describe transient phenomena. Using these parameters, we have fit spectra of mixed nitride phases during decomposition in hydrogen and helium.

The spectra of γ'–Fe_4N is characterized by the overlap of two sets of six line patterns, Fe-I (0nn - zero nearest neighbors) and Fe-II (2nn). The outermost velocity peak of Fe-I (5.71 mm/s) does not overlap with peaks from iron or other nitrides and clearly indicates the presence of this phase. Fe-II (2nn) can be adequately fit with a single set of six lines, but an improved fit is found for a pair of lines IIA and IIB.

For ϵ–Fe_xN $(2 < x < 3)$ a distribution of sites from 0 nearest neighbors to 3 nearest neighbors makes for at least a 24 line fit. The hyperfine fields at 2nn or 3nn were found to vary linearly with nitrogen content. An additional quadrupole doublet Fe-Q included in the fits of these spectra is attributed to a ζ–Fe_2N precursor.

The single phase orthorhombic nitride, ζ–Fe_2N, is characterized by an intense paramagnetic doublet down to 4.2K. The fits of these spectra also require small contributions from Fe-Q.

Fits of the spectra taken during the decomposition of ζ–Fe_2N at 473 K indicate that a shrinking core model is appropriate. Decomposition in helium is not significant until about 600 K. Mössbauer fits indicate that a γ'–Fe_4N sample lost 50% of the original phase after a 1 1/2 hr treatment at this temperature.

Transient kinetics work in this period has emphasized an examination of the possibility of moderating nitrogen loss from iron nitrides by precoating the surface with carbon. Exposing ζ–Fe_2N to CO for 1 minute at 573°K does deposit carbon on the surface. The presence of the carbon produces an induction period before NH_3 is released from the catalyst upon subsequent exposure to $3H_2/CO$ synthesis gas. Thus the moderation effect of carbon does not appear to have the desired selectivity.

2.2 Mössbauer Spectroscopy

Mössbauer studies of the iron nitrides have been an important part of this research from the beginning. In past reports we have shown spectra for all of the thermodynamically stable nitride phases and discussed their stability. In order to examine the conversion of phases during reaction quantitatively, we need precise analysis of the spectra. The curve fitting of the nitrides is now completed and we report here the analysis of the pure phases and their stability in H_2 and He.

γ' Fe_4N

The characterization by Mössbauer spectroscopy of the γ 'nitride by other investigators has been discussed previously (1). The γ'–Fe_4N spectrum (Figures 1c and 2) is identified by a characteristic eight line pattern of approximate peak intensities 1:2.5:1.5:1.0:1.0:1.5:2.5:1 arising from an overlap of Fe-I (0nn - zero nitrogen nearest neighbors and Fe-II (2nn) fields. The higher 0nn hyperfine field (340 kOe) is attributed to iron atoms at the corner of a unit cube. The peak positions of this 6 line pattern are located at -5.24, -2.94, -0.64, 1.10, 3.41, and 5.71 mm/s. As such, the most positive velocity peak (5.71 mm/s) does not overlap either with iron or with peaks from other nitrides and often serves to indicate the presence of γ'–Fe_4N in complex, overlapping spectra. The lower 2nn hyperfine field (215 kOe), attributed to iron atoms at the face center of a unit cube, has approximate peak positions of -3.20, -1.72, -0.42, 0.84, 2.32, and 3.80 mm/s. Although three times the area of the 340 kOe splitting, the 2nn field

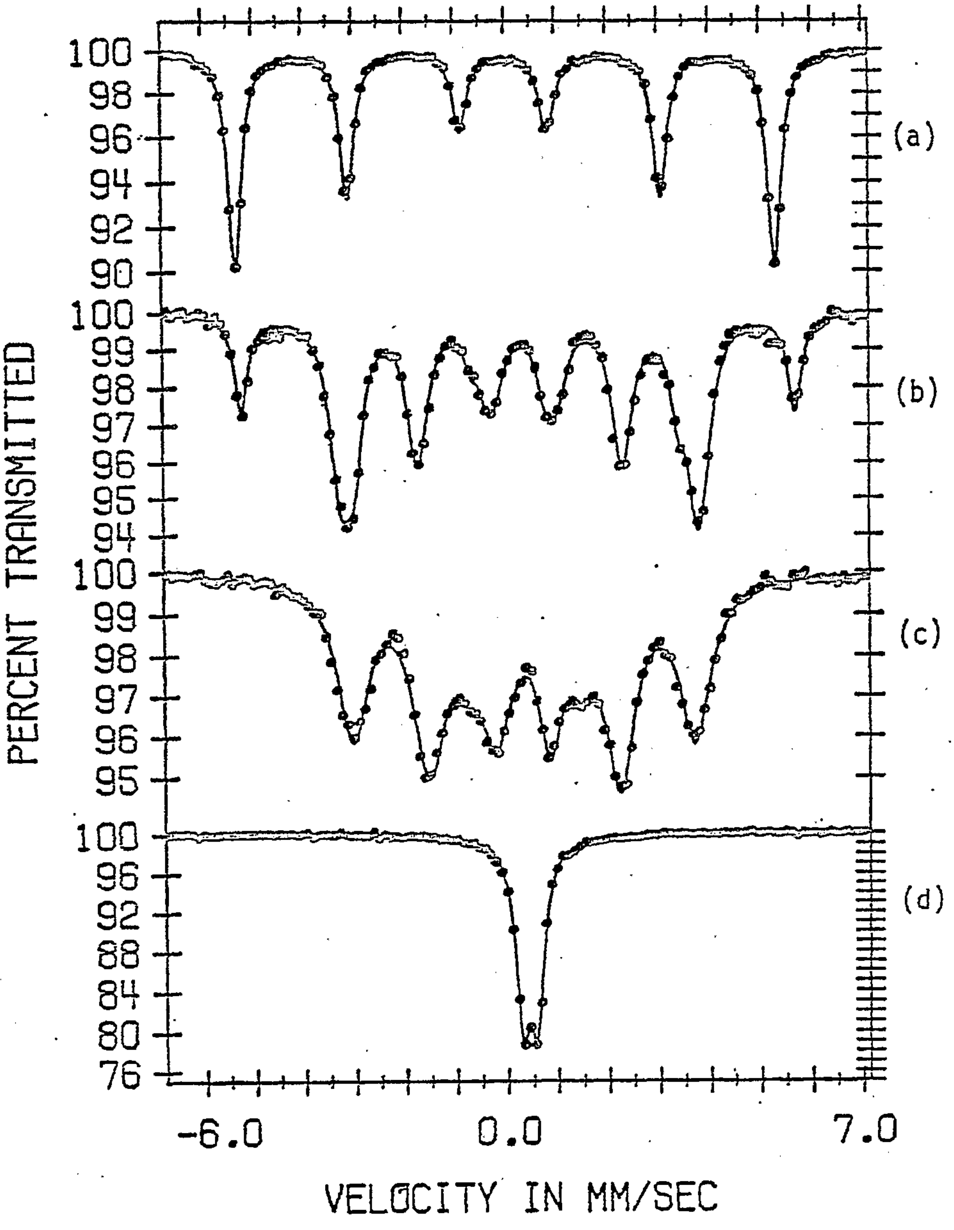

Figure 1 Mössbauer Spectra of Single Phase Nitrides.

a) α -Fe
b) γ'-Fe_4N
c) ε -$Fe_{2.52}N$
d) ζ -Fe_2N

TABLE 1

Mössbauer Parameters (298 K) of Single Phase Nitrides

Phase	Figure	Iron Identity	IS (mm/s)	QS (mm/s)	HFS (kOe)	LW (mm/s)	RA (%)	Total Area
α-Fe	1a	α-Fe	0.00	0.00	329.4		100.0	.2151
γ'-Fe_4N	1b (2b)	γ'-I	0.23	0.00	339.4		22.2	.2317
		γ'-IIA	0.29	-0.14	218.1		49.9	
		γ'-IIB	0.31	-0.34	215.4		25.0	
		Fe-Q	0.29	1.37	---		2.9	
ε-$Fe_{2.52}N$	1c (3a)	ε-II	0.33	0.00	209.0	0.73	61.2	.2858
		ε-III	0.41	0.00	112.4	0.65	30.4	
		Fe-Q	0.32	1.15	---	0.53	8.2	
ε-$Fe_{2.39}N$	3b	ε-II	0.33	0.00	195.7	0.70	48.5	.2778
		ε-III	0.43	0.00	103.4	0.73	36.2	
		Fe-Q	0.37	1.10	---	0.92	18.3	
ε-$Fe_{2.33}N$	3c	ε-II	0.32	0.00	189.5	0.73	42.2	.2746
		ε-III	0.43	0.00	99.7	0.72	29.9	
		Fe-Q	0.35	0.97	---	0.83	27.9	

TABLE 1 (Continued)

Phase	Figure	Iron Identity	IS (mm/s)	QS (mm/s)	HFS (kOe)	LW (mm/s)	RA (%)	Total Area
ε-$Fe_{2.25}N$	3d	ε-II	0.31	0.00	171.2	0.90	33.4	.2830
		ε-III	0.44	0.00	88.5	0.79	28.5	
		Fe-Q	0.36	0.87	---	0.90	38.1	
ε-$Fe_{2.14}N$	3c	ε-II	0.28	0.00	161.6	0.96	19.8	.2733
		ε-III	0.46	0.00	78.0	1.07	33.3	
		Fe-Q	0.34	0.68	---	0.93	59.9	
ζ-Fe_2N	1d	ζ-II	0.43	0.28	---	0.35	100.0	.1813

overlaps with ϵ -nitride and χ–Fe_5C_2 generated fields. The 0nn site has an isomer shift relative to α -iron of 0.24 mm/s and does not exhibit a quadrupole splitting. These findings are in excellent agreement with previous investigators (Table 1).

We turn to Figure 2 to resolve the identity of the 2nn field. Clauser (2) proposed that the 215 kOe field was neither due to a single site nor due to two electronically different environments. Rather, sites IIA and IIB were on adjacent faces of the unit cube. Ideally site IIA should be twice as intense as IIB and have a quadruople splitting half in magnitude and of opposite sign to that of IIB. Figure 2 presents two different γ' nitride samples each fitted with one 2nn site (2a, 2c) and then again with the IIA and IIB sites (2b, 2d). Both phases were synthesized from α -Fe by nitriding in 80% NH_3 at 623 K. The three magnetic field simulation provides better fit statistics. The IIA site area is fixed as twice the IIB area by equating all widths in each site and by constraining the peak intensities to a 2:1 ratio. Within each sextet, the intensities are constrained to 3:2:1:1:2:3. In order to maintain correct peak symmetry, the energy difference between peaks 2 and 3 is equated to the difference between 4 and 5. The quadrupole splitting is left unconstrained. The ratio QS_A:QS_B is -.41:1 in Figure 2b and is -.35:1 in Figure 2d. This is sufficiently close to the predicted -0.5:1 value.

On the basis of an improved fit and a correlation to physical predictions, γ'–Fe_4N spectra are fitted more correctly with IIA and IIB sites. In spectra with several phases, however, one is unable to make this distinction. The γ' nitride nitride contribution is then fit to the 0nn site and a single 2nn site.

ε-Fe_xN

The hexagonal close packed nitrides are less straightforward to characterize by Mössbauer spectroscopy than the γ'-nitrides. The variation in hyperfine field for individual iron sites with changing composition does not permit distinguishing ε-nitrides by the velocity of certain peaks. Rather, we consider separate nearest nitrogen configurations for each iron site whose hyperfine field is reduced from a base value in direct proportion to the concentration of nitrogen within the nitride. As each iron atom in the hcp lattice has six nearest octahehral intensities, only three of which may be occupied by nitrogen, we consider at most four magnetically ordered ε sites: 0nn, 1nn, 2nn, and 3nn. The magnetic fields among these sites increase in the order $H_3 < H_2 < H_1 < H_0$. Quadrupole splittingsare not apparent in ε-nitride spectra.

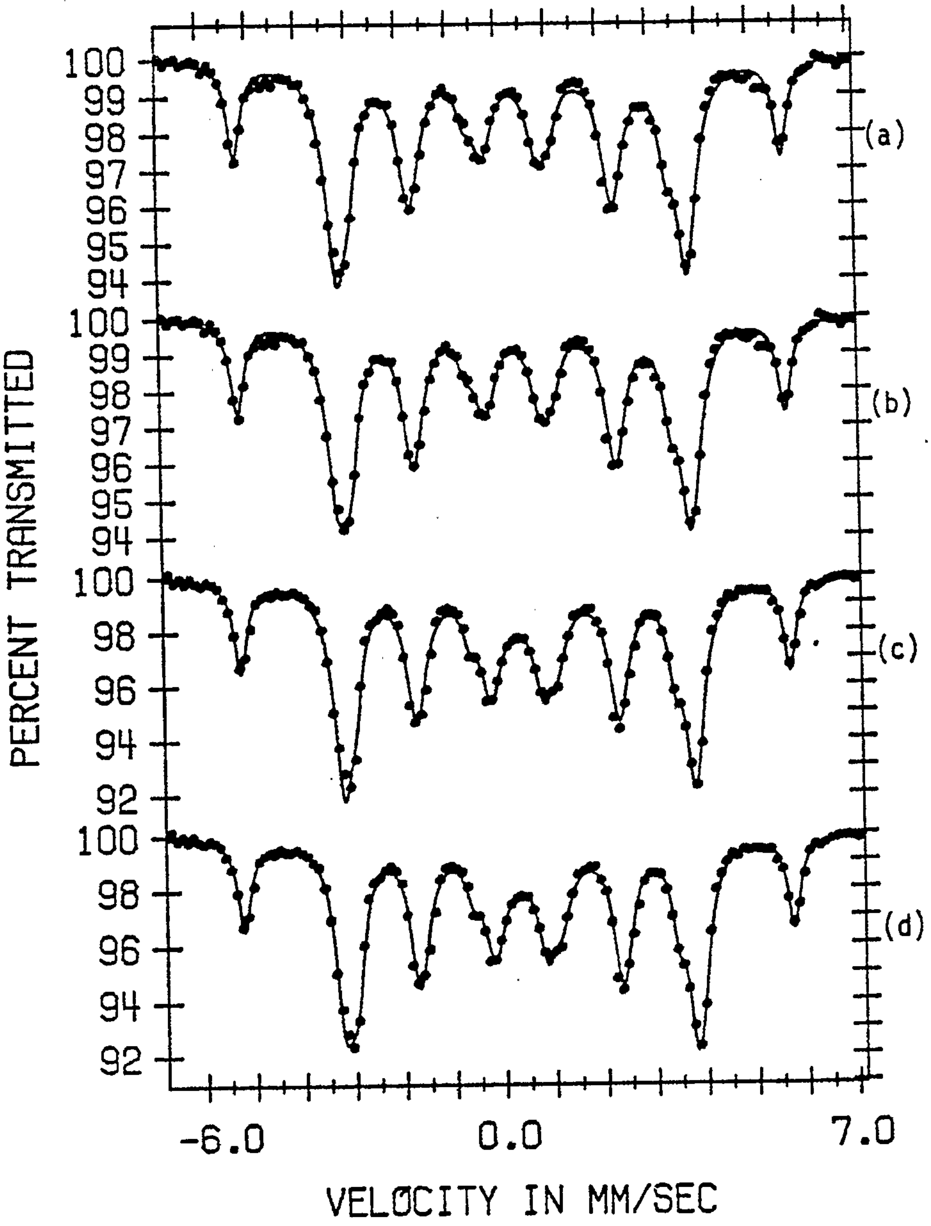

Figure 2 Mössbauer Spectra of γ'-Fe_4N.

a) nitrided in 80% NH_3 at 598 K (14 peak fit)

b) as above (20 peak fit)

c) γ'-Fe_4N treated in He at 523 K (14 peak fit)

d) as above (20 peak fit)

LeCaer et al. [3] reported that the distribution of nearest neighbor sites in a close packed (hcp of fcc) interstitital compound determines the nominal stoichiometry of the material. An estimate of the interstitial nitrogen content in the ε-nitrides can be made from equation 1. Figure 3 shows the spectra of five epsilon nitrides of increasing nitrogen content, as estimated from equation 1. The highest N containing nitride (Figure 3e) was produced by nitriding a reduced iron powder with 91% NH_3 in H_2 at 673 K for 5.5 hr. This sample was then treated at progressively lower temperatures to produce ε-nitrides lower in N content (3d-b). The nitride in Figure 3a was synthesized in 90% NH_3 at 598 K for 6 hours. Computer fits of these spectra were generated by considering two hyperfine fields and a nonmagnetic quadrupole split component. Peak widths within a sextet were constrained equal and peak intensities were held to 3:2:1:1:2:3. The Mössbauer parameters are given in Table 1. The field with larger splitting and lower isomer shift is attributed to the two nitrogen neighbor site, ε-II. The second is attributed to ε-III, the 3nn site. These parameters are in accordance with reported literature assignments (Table 1).

The nonmagnetic component, Fe-Q, fitted with equal width and equal intensity constraints, is seen to vary in quadrupole splitting from 1.15 mm/s in Figure 3a to 0.68 in Figure 3e. The average isomer shift values fluxuate around 0.35 mm/s. The component is unlikely to be an oxide species because of the reducing nature of the nitriding environment. The oxide precursor can be nitrided even in pure ammonia at 473 K. Two, more plausible explanations are considered. The first

Figure 3 Mössbauer Spectra of ε-Fe_xN.

a) nitrided in 90% NH_3 at 598 K for 6 hours
b) nitrided (c) treated in 91% NH_3 at 523 K for 6 hours
c) nitrided (d) treated in 91% NH_3 at 553 K for 6 hours
d) nitrided (e) treated in 91% NH_3 at 598 K for 6 hours
e) nitrided in 91% NH_3 at 673 K for 6 hours

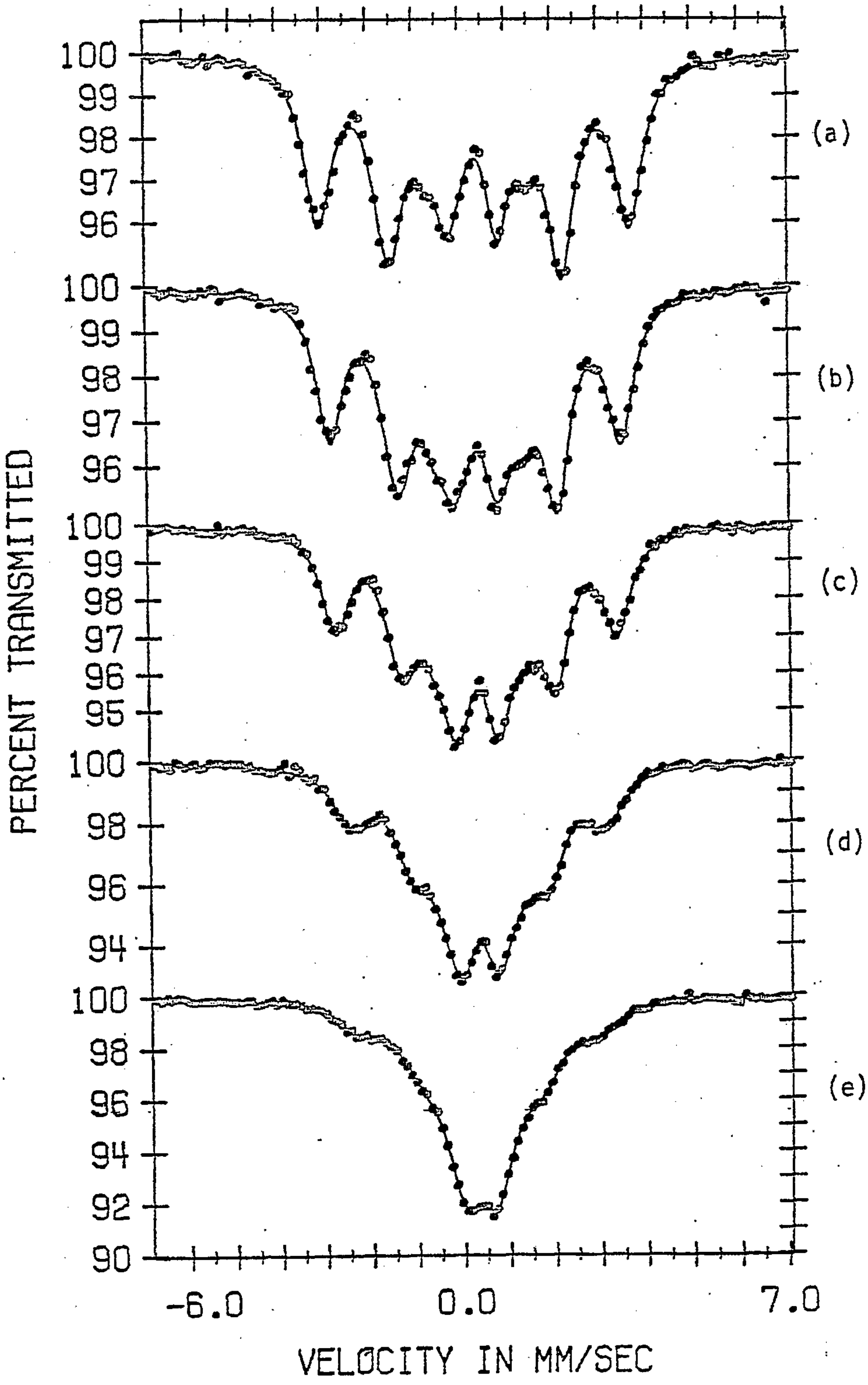
100
99
98
97
96
(a)
100
99
98
97
96
(b)
100
99
98
97
96
95
(c)
100
98
96
94
(d)
100
98
96
94
92
90
(e)
PERCENT TRANSMITTED
-6.0
0.0
7.0
VELOCITY IN MM/SEC

Figure 3

attributes this species to the transition nitride of ζ-Fe_2N, a three nearest nitrogen neighbor site whose Curie temperature has fallen below room temperature with the increase in nitrogen content. The QS of this species slowly decreases and at higher nitrogen contents may approach that of ζ-Fe_2N (0.28 mm/s). The second explanation attributes the species to a casualty of the fitting technique. Chen et al. [4] analyze their ε-nitride phases with a distribution of hyperfine fields, the innermost two peaks being relatively intense, but narrow, and the outermost peaks severely broadened; so much so, that the intensities of the middle two peaks (2 and 5) are often more than the outermost. Yeh et al. [48], however, even when using this approach require a central doublet which can account for 20% of the spectral area. The variable width approach is physically correct in accounting for higher than first neighbor interactions and from Figure 3 we see that the equal width constraint is creating slightly too wide a theoredical fit to ε-II peaks 2 and 5, i.e. a larger width is biased by the greater areas of the two outermost ε-II peaks. Nonetheless, the close computer fits obtained with the equal width and 3:2:1:1:2:3 intensity constraints indicates that the second and higher nearest neighbor effects are small in large, unsupported iron nitride particles and that this approach is still valid.

The average stoichiometry of the ε-nitrides is estimated from the spectral areas of each of the three components, assuming equal recoil free fractions and 3nn Fe-Q composition. The composition range in Figure 3 is then from $Fe_{2.52}N$ to $Fe_{2.14}N$. The magnitude of hyperfine splitting of the ε-II and ε-III sites in these nitrides is correlated against the composition parameter x in Fe_xN (see Figure 4). A linear regression analysis for a linear variation of field strength with composition gives the ε-II and ε-III correlations, with correlation coefficients of 0.99, in equations 2 and 3 respectively.

$$H_{II} = -119.4 + 131.0 \cdot x \quad (\text{kOe}), \quad 2.1 < x < 2.6 \qquad (2)$$

$$H_{III} = -118.6 + 92.4 \cdot x \quad (\text{kOe}), \quad 2.1 < x < 2.6 \qquad (3)$$

These correlations serve as a prediction of approximate phase stoichmetry for the ε-nitrides. The correlation becomes meaningless in nitrides approaching Fe_2N stoichiometry due to the rapid fall in Curie temperature.

ζ-Fe_2N

The single phase orthorhombic nitride, ζ-Fe_2N, is characterized by a Mössbauer spectrum with an intense paramagnetic doublet down to 4.2 K. The room temperature spectrum (Figure 1d) has absorption peaks at 0.29 and 0.57 mm/s, corresponding to an isomer shift of 0.43 mm/s and a quadrupole splitting of 0.28 mm/s. The zeta-nitride is readily prepared from reduced iron prowder by nitriding in pure ammonia at temperatures above 473 K. Extended nitriding is often required to produce an homogeneous phase. Figure 5 illustrates this requirement. The sample in Figure 5a was nitrided in 93% ammonia at 673 K for 3 hours and then nitrided in pure NH_3 at 623 K for an additional hours (Figure 5b). Although both samples are computer fit with an Fe-Q (IS = 0.32 mm/s, QS = 0.44-0.45 mm/s) contribution the additional hour of nitriding has clearly increased the spectral resolution of the

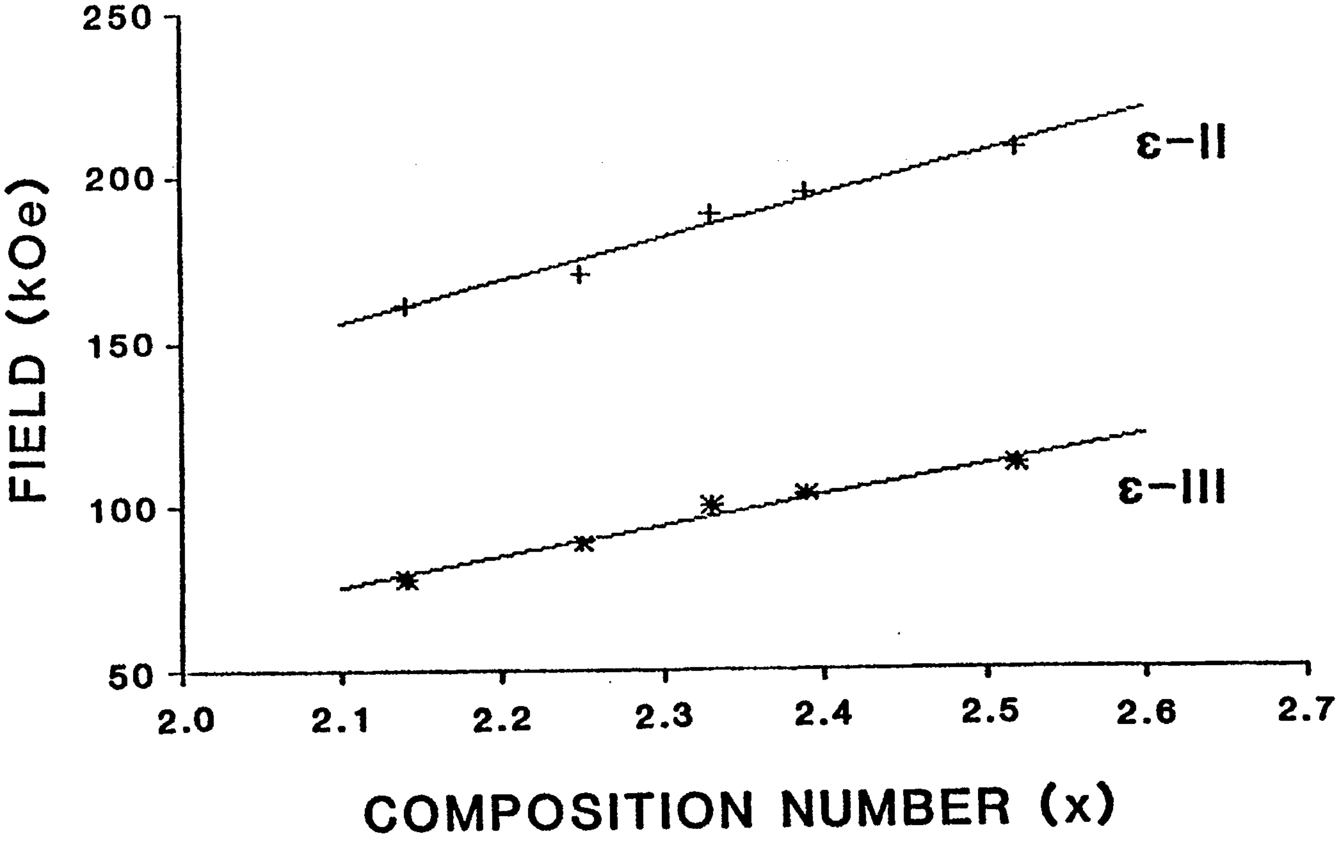

Figure 4 Variation in Magnetic Splitting with ε-Nitride Composition

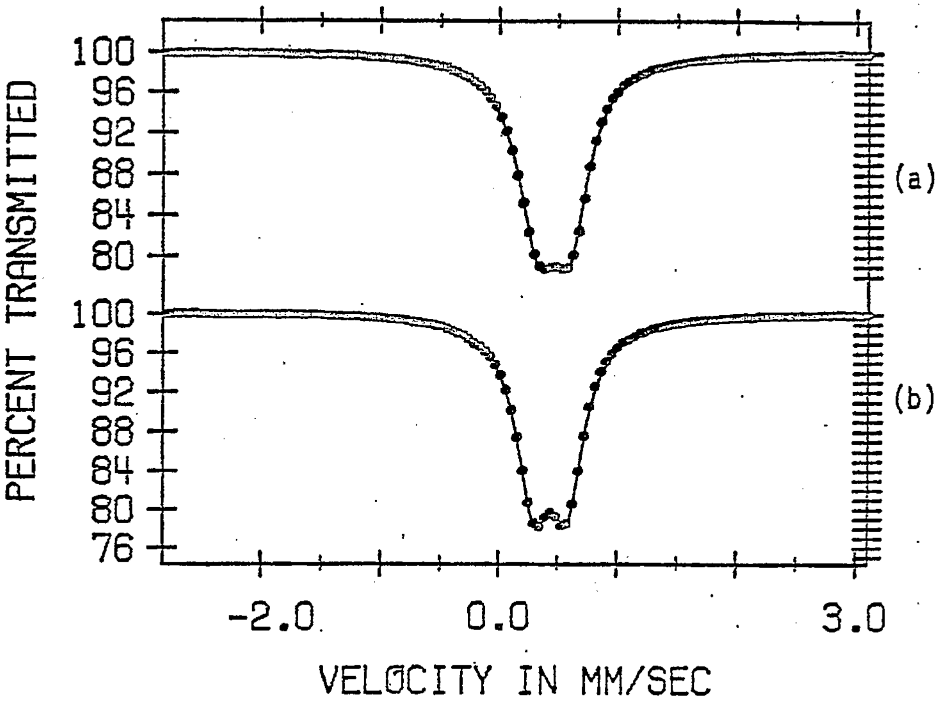

Figure 5 Mössbauer Spectra of ζ-Fe_2N.

a) nitrided in 93% NH_3 at 673 K for 3 hours

b) treated in 100% NH_3 at 623 K for 1 hour zeta phase. The pure ζ-Fe_2N spectrum shown in Figure 1d was in fact annealed in He for four hours after nitriding in 100% NH_3 at 523 overnight.

STABILITY

H_2/NH_3

The stability of the bulk nitride phases in hydrogen and hydrogen/ammonia mixtures is discussed. Jack [5], Bridelle [6], and Anderson [7-9] noted extreme nitride instability in H_2. Mössbauer spectra confirm that even the dense orthorhombic nitride loses all its nitrogen within the first twenty minutes of exposure to H_2 at temperatures above 523 K. Figure 6 compares the rate of loss of ζ-Fe_2N in H_2 to the loss in other gas atmospheres. Constant velocity spectra follow the decrease in intensity (rise in % counts) of the more positive ζ-Fe_2N peak with time. The rapid loss of Fe_2N phase in H_2 and $3H_2/CO$ environments is evident from these spectra. In an effort to slow the denitriding rate in H_2 sufficiently so as to observe intermediate nitride phases, a ζ-Fe_2N specimen was exposed to 100% H_2 at 473 K for several minutes. Figure 7 shows how a reduction in denitriding temperature from 623 to 473 K slows the loss of Fe_2N, as measured by constant velocity transients. The phase loss, although still rapid, is slow enough to premit constant acceleration spectra to be helpful.

Figure 8 illustrates the sequential 473 K denitriding of a ζ-Fe_2N sample. Hydrogen at 100 ml/min flows for 2.5, 5.0, 10.0, and 21.0 minutes in Figure 8 a-e respectively. After each exposure at 473 K, heating is stopped and liquid nitrogen is poured into the center of

Figure 6 In Situ Analysis of ζ-Fe_2N Stability at 523 K.

a) step change to H_2 from NH_3
b) step change to He from NH_3
c) step change to $3H_2/CO$ from NH_3
d) step change to CO from NH_3
e) step change to $3H_2/CO$ from NH_3 over pre-oxidized ζ-Fe_2N

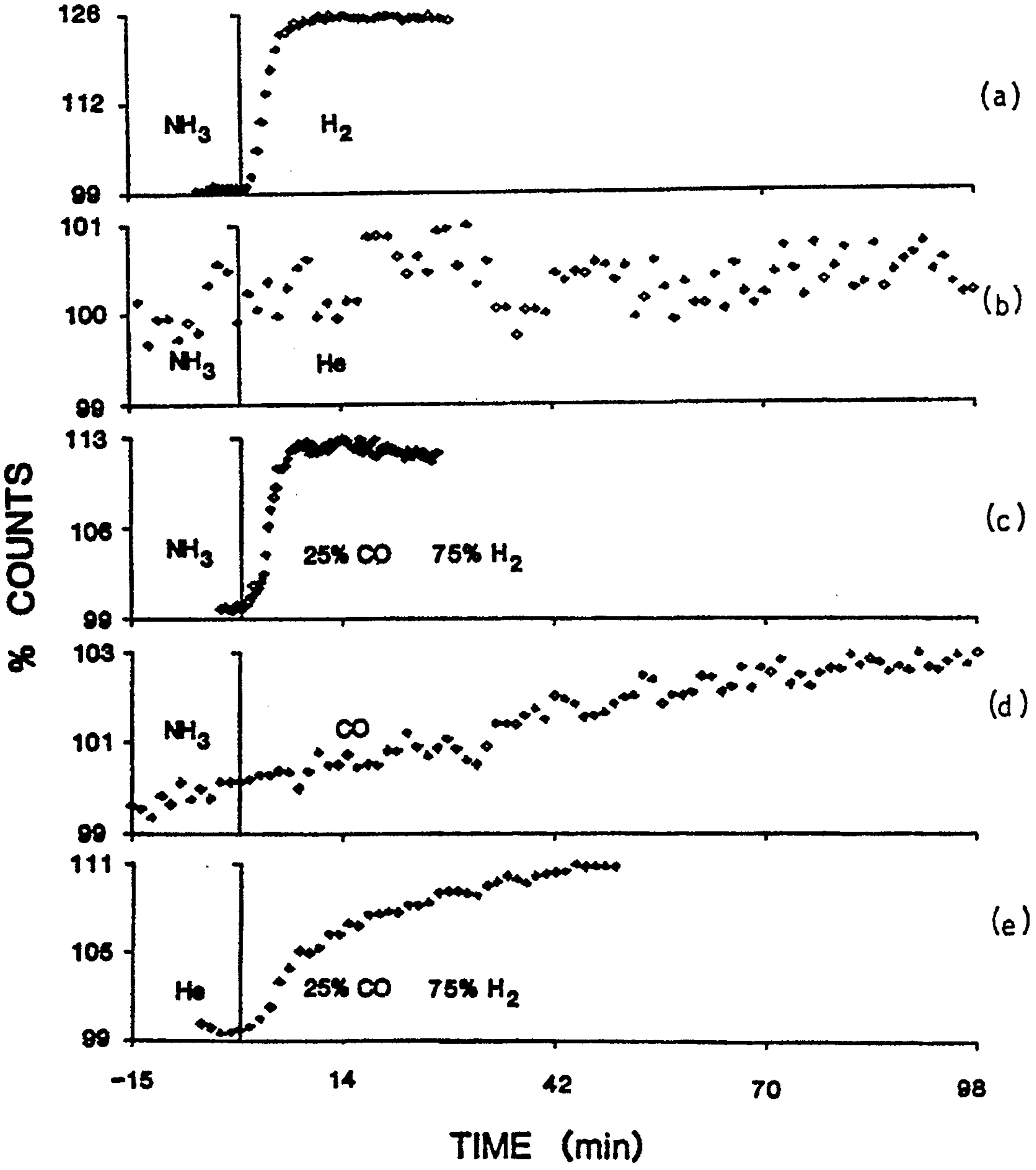
126
112
99
NH$_3$
H$_2$
(a)
101
100
99
NH$_3$
He
(b)
113
106
99
NH$_3$
25% CO 75% H$_2$
(c)
% COUNTS
103
101
99
NH$_3$
CO
(d)
111
105
99
He
25% CO 75% H$_2$
(e)
-15
14
42
70
98
TIME (min)

Figure 6

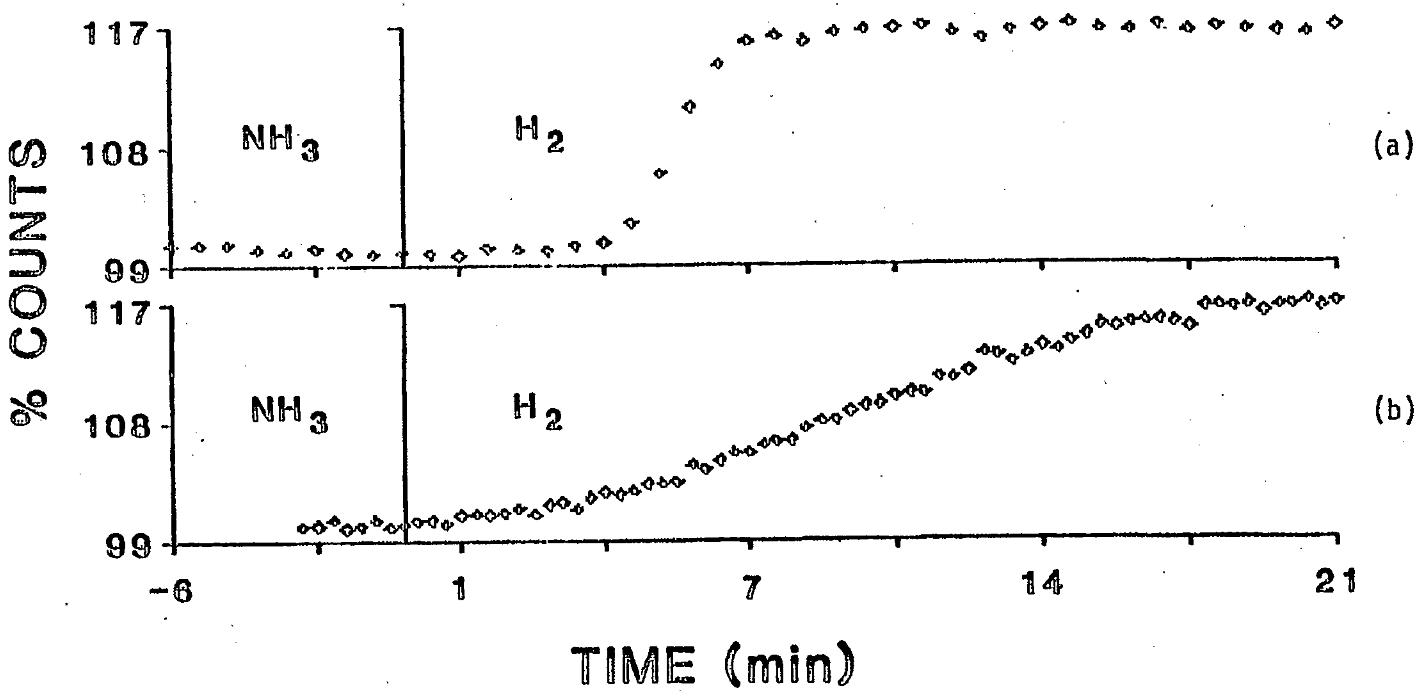

Figure 7 *In Situ* Analysis of ζ-Fe_2N Denitriding.

a) step change to H_2 from NH_3 at 598 K

b) step change to H_2 from NH_3 at 473 K

Figure 8 Mössbauer Spectra of Partly Denitrided ζ-Fe_2N.

a) treated in H_2 at 473 K for 2.5 minutes
b) treated in H_2 at 473 K for 5.0 minutes
c) treated in H_2 at 473 for 10 minutes
d) treated in H_2 at 473 for 10 minutes (liquid nitrogen spectrum)
e) treated in H_2 at 473 for 21 minutes

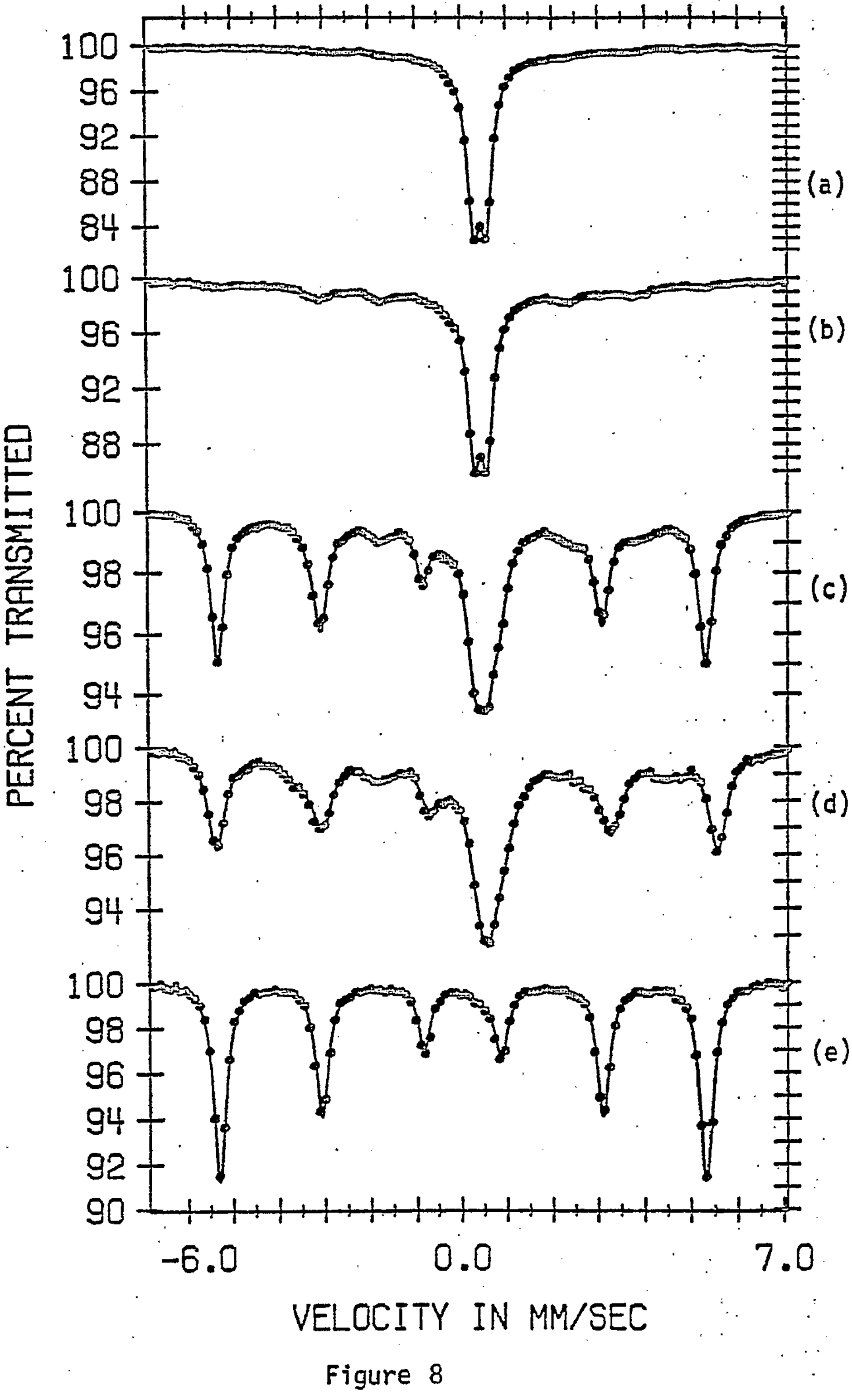
100
96
92
88
84
(a)
100
96
92
88
(b)
100
98
96
94
(c)
100
98
96
94
(d)
100
98
96
94
92
90
(e)
PERCENT TRANSMITTED
-6.0
0.0
7.0
VELOCITY IN MM/SEC

Figure 8

The annular cell housing. The catalyst wafer is exposed to 373+ K hydrogen atmosphere only for several additional minutes. The spectral parameters (Table 2) for Figure 8a confirm that the Fe_2N sample did not undergo noticeable phase reordering during a 2.5 minute H_2 treatment. Only two doublets, a ζ-nitride and a non-magnetic Fe-Q contribution, are present in the spectrum. The lag time associated with the manifold dead volume and CSTR mixing characteristics of the reactor cell, decreases the nominal 2.5 minute treatment to a sub-minute exposure. Figure 8e illustrates the other extreme; after 21 minutes exposure to H_2, denitriding is virtually complete. The spectrum is 95% Fe but exhibits a noticeable broadening of the +0.85 mm/s peak. This asymmetry can be corrected by including a doublet with isomer 0.44 mm/s and quadrupole splitting 0.27 mm/s. These parameters, considering the starting Fe_2N material, clearly indicate residual ζ-nitride. The locally homeogeneous mature of denitriding is more easily seen from intermediate H_2 exposures.

Figure 8b presents the spectrum of a ζ-Fe_2N sample after 5 minutes in hydrogen. The paramagnetic ζ peaks are lower in intensity than after 2.5 minutes in H_2. Magnetically ordered sites are clearly present in addition to ζ and Fe-Q, and are seen more clearly by subtracting the four non-magnetic peaks (Figure 9). Computer fitting reveals two sites: one with IS = -0.01 mm/s and 329.4 kOe field, and a second with IS = 0.32 and HFS = 214.2 kOe. The higher field site could not be fit with a magnetic splitting above 330 kOe. The isomer shift of ~0 mm/s identifies this site as α-Fe. Nitrogen solubility in

TABLE 2

Mössbauer Parameters of Non-equilibrium Nitrides

Figure	Iron Identity	Temp (K)	IS (mm/s)	QS (mm/s)	HFS (kOe)	LW (mm/s)	RA (%)	Total Area
8a	Fe-Q	298	0.39	0.18	---	5.25	41.9	.2324
	ζ-Fe_2N		0.44	0.28	---	0.35	58.1	
8b	α-Fe	298	-0.01	0.00	329.4	0.54	4.9	.2789
	2nn		0.32	0.00	214.2	0.75	9.7	
	Fe-Q		0.37	0.72	---	6.49	47.7	
	ζ-III		0.44	0.29	---	0.34	37.7	
8c	α-Fe	298	0.01	-0.01	328.8	0.36	51.4	.2129
	2nn		0.28	+0.19	221.4	0.81	16.7	
	ζ-III		0.44	0.27	---	0.47	28.1	
	unknown		(0.62)	(0.00)	(138.7)	(0.39)	(3.8)	
8d	α-Fe	85	0.10	0.00	338.1	0.48	44.0	.2478
	2nn		0.43	+0.13	247.1	0.86	20.5	
	ζ-III		0.52	0.19	---	0.64	29.5	
	unknown		(0.90)	(0.00)	(160.4)	(0.52)	(6.0)	
8e	α-Fe	298	0.00	+0.01	329.6	0.34	95.0	.2376
	ζ-III		0.44	0.27	---	0.85	5.0	

TABLE 2 (Continued)

Figure	Iron Identity	Temp (K)	IS (mm/s)	QS (mm/s)	HFS (kOe)	LW (mm/s)	RA (%)	Total Area
10a	γ'-I	298	0.24	0.00	340.3	0.51	8.5	.2222
	γ'-II		0.30	+0.04	218.0	0.41	29.6	
	ζ -III		0.43	0.28	---	0.36	31.2	
	Fe-Q		0.37	0.05	---	2.29	30.7	
10c	γ'-I	298	0.20	0.00	342.4	0.60	4.0	.2307
	γ'-II		0.31	+0.01	216.4	0.42	18.5	
	ζ -III		0.43	0.29	---	0.38	39.3	
	Fe-Q		0.36	0.06	---	2.53	38.2	

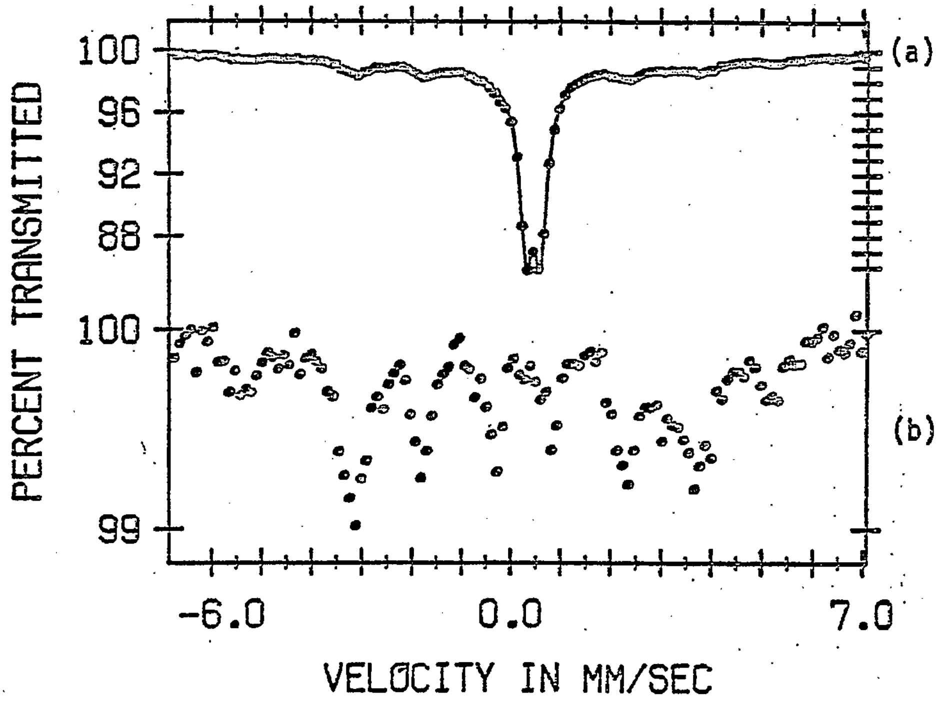

Figure 9 Mössbauer Spectra of Partly Denitrided ζ-Fe_2N Intermediate.

a) treated in H_2 at 473 for 5 minutes

b) spectrum (a) less ζ-Fe_2N and Fe-Q contributions the matrix is likely. The 2nn site (214.2 kOe) cannot be categorically attributed to either ε-II or γ'-II on the basis of its Mössbauer parameters. The existence of a small concentration of either a γ' 0nn site or an ε-III contribution cannot be denied with the present spectral resolution.

After 10 minutes of H_2 exposure (Figures 8 c-d), the coexistence of α-Fe and ζ-Fe_2N is easily seen. The room and 85 K temperature spectra are computer fitted with α-Fe, 2nn, and ζ-III contributions. The quadrupole splitting of the 2nn site is unconstrained so as not to bias the spectral analysis. Even with fixing the 2nn QS to zero, a third, unknown magnetic site (140-160 kOe) is still needed to fit these spectra. Again a γ'-0nn site is not seen in either spectra, as the most positive velocity iron peaks are symmetric and equal in intensity to the corresponding negative velocity peaks. The 2nn site is then more likely to arise from an hexagonal nitride structure than a cubic nitride. In these spectra the distribution of nitrogen through the nitride lattice will be more asymmetric than in homogeneous nitrides, as the rapid rate of N removal does not permit equilibration. The positive QS for the 2nn site and the diffuse nature of the unknown site (140-160 kOe) could be visualized as an inhomogeneity within the transition nitride structure. The increase in 'nitride phase' spectral area from the room temperature to 85 K spectrum (because the nitride recoil free fraction is below that of the α-Fe) indicates that the iron content of this specimen is below 44%.

A pathway for ζ-Fe_2N formation from reduced iron is suggested from Figure 10. The Mössbauer spectra of iron powder nitride in 100% NH_3

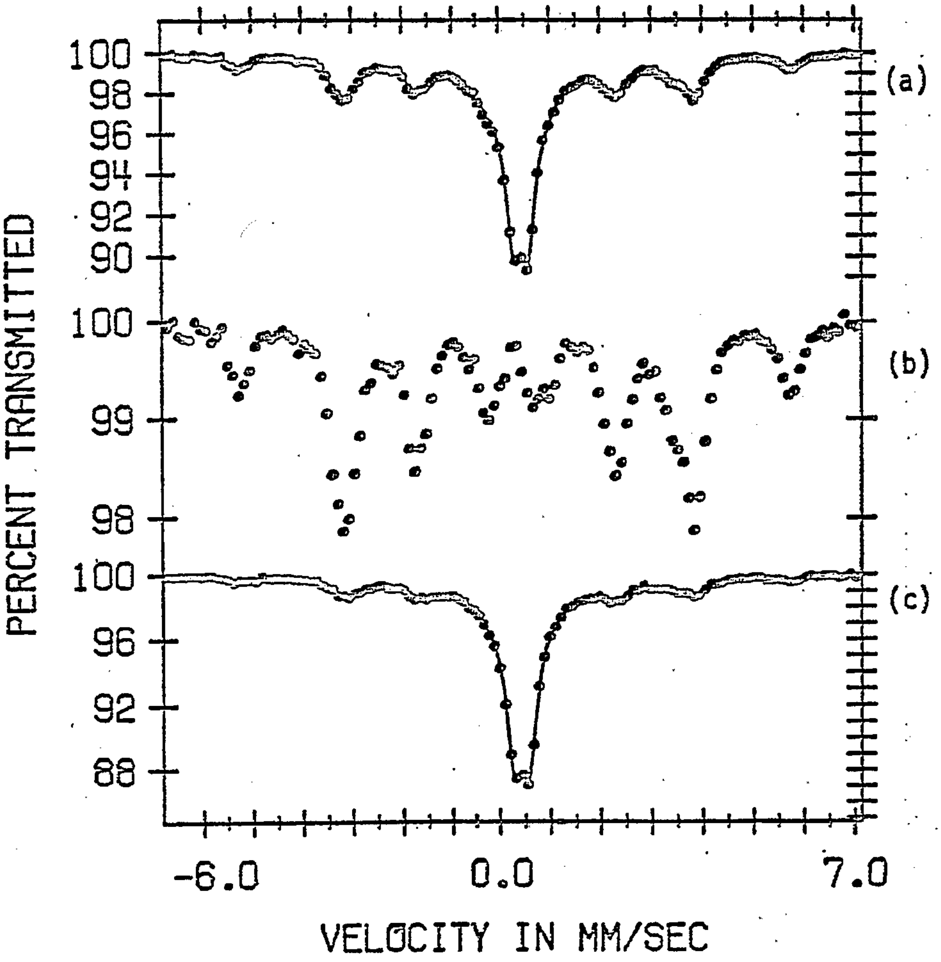

Figure 10 Mössbauer Spectra of Partly Nitrided α-Fe.

a) treated in NH_3 at 498 K for 3 hours

b) spectrum (a) less ζ-Fe_2N and Fe-Q contributions

c) treated in NH_3 at 473 K for 11 hours at 498 K for 3.5 hours (Figure 10a) and powder nitrided in pure ammonia at 473 K for 11 hours (Figure 10c) contain γ'-Fe_4N and ζ-Fe_2N contributions. The two magnetic sites in Figure 11a are fitted to 340.3 kOe (IS = 0.24 mm/s) and 218.0 kOe (IS = 0.30 mm/s) sites, with areas 8.5 and 29.6%, respectively. These parameters (Table 2) are in accordance with γ'-nitride. Subtracting the 4 non-magnetic peaks produced Figure 10b which shows the γ'-Fe_4N transition nitride more clearly. The two magnetic sites in Figure 10c are similarly attributed to γ'-nitride. The lower γ'-Fe_4N spectral % for the 473 K nitrided powder makes fitting of the 0nn site imprecise. Unconstrained fits, however, do not indicate any α-Fe contribution in this region, nor could the hyperfine field isomer shift be successfully constrained to that of α-Fe. The slightly larger than expected 2nn:0nn spectral area ratio may be due to a ε-2nn nitride. Indeed, as the iron nitride phase diagram provides no conditions under which γ'- and ζ-nitrides are in equilibrium, some bridging structure (ε-nitride) is expected.

Two factors influence the difference in "transition nitride" assignment during iron powder nitriding versus Fe_2N denitriding. Firstly, the different time scales for Fe_2N formation versus decomposition are important. Rapid denitriding at temperatures as low as 473 K is likely to promote interstitial N inhomogeneity. Figure 11 illustrates via constant velocity measurements, the slow growth, when compared to Figure 7 of the Fe_2N phase. Secondly, the diffusivity of nitrogen through the lattice is slower through the denser (high N content) nitrides, and substantially faster through α-Fe. A $\gamma'Fe_4N$

Figure 11 *In Situ* Analysis of α-Fe Nitriding.

a) step change to NH_3 from H_2 at 598 K
b) step change to NH_3 from H_2 at 523 K
c) step change to NH_3 from H_2 at 473 K

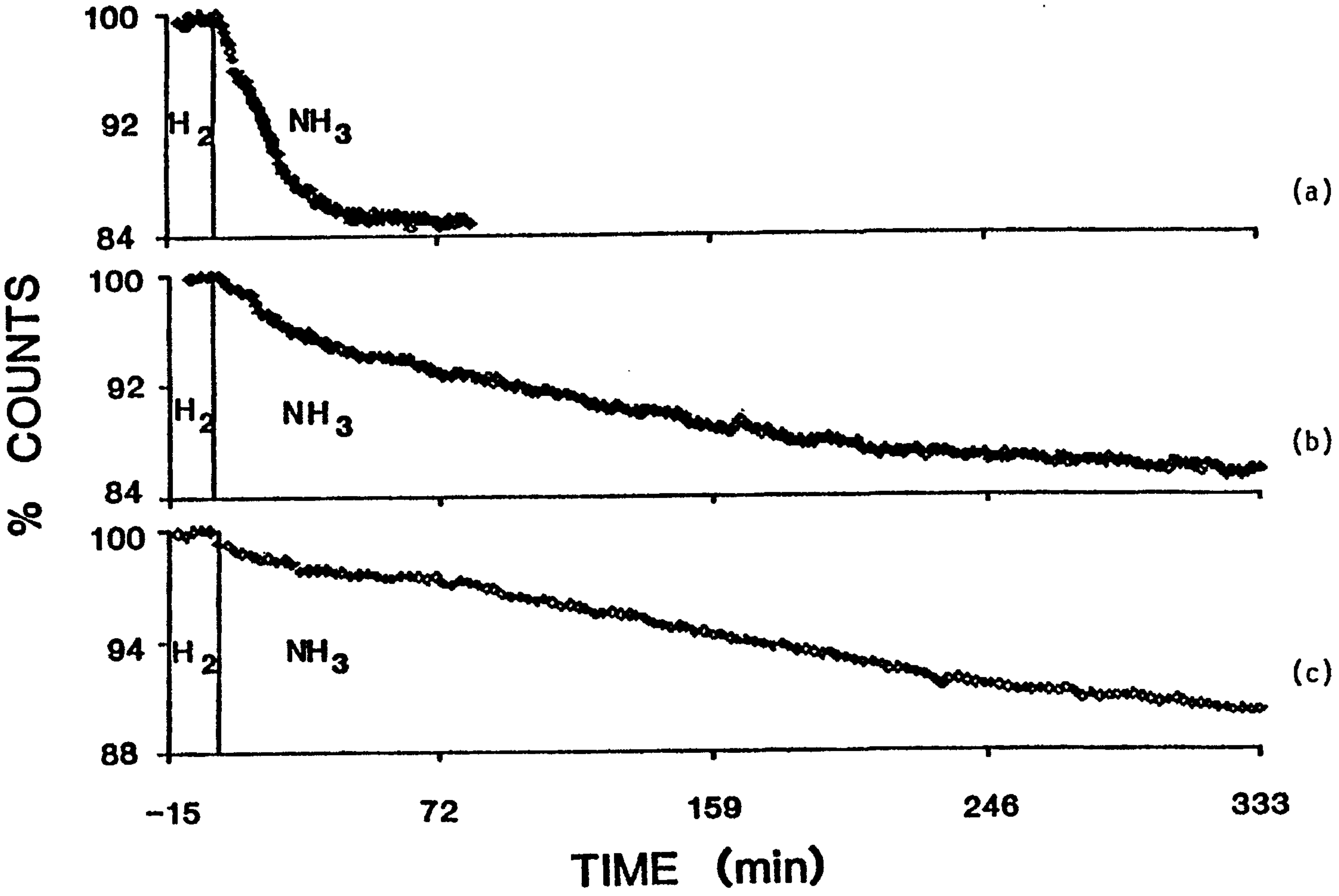
100
92
84
H 2
NH 3
(a)
100
92
84
H 2
NH 3
(b)
100
94
88
H 2
NH 3
(c)
% COUNTS
-15
72
159
246
333
TIME (min)

Figure 11

intermediate then, once denitrided slightly to Fe, is expected to lose N very rapidly in H_2 atmospheres. If, for example, the Fe_2N denitriding occurs via a banded, shrinking nitride core, with an α-Fe surface and progressively richer nitrogen nitride phases toward the particle center, the nitride layer (γ') adjoining the α-Fe will be narrow and small in volume. This resulting steep N concentration gradient must be decreased in order to determine a likely "transition phase". Either a further denitriding temperature reduction, or a lowering of H_2 partial pressure would be necessary.

He

The nitrides are essentially stable in helium, but thermal decomposition via N_2 is activated at sufficiently high temperatures. The degree of this activation at 523 K is estimated by comparing constant acceleration spectra of the nitride phases before and after He exposure. The dynamics of the bulk change of ζ-Fe_2N in He are shown by a constant velocity measurement in Figure 6. Despite the scatter in this data, it is evident that no significant bulk phase transformation has occured. The constant acceleration spectrum (Figure 1d) of this ζ-Fe_2N sample after 3.5 hours He at 523 K indicates the presence of only zeta nitride. No Fe-Q contribution could be accomodated in the fit. The isothermal bake may have assisted in structurally transforming Fe-Q to zeta nitride, as a more pure Fe_2N phase has not been produced by nitriding alone. Some nitride decomposition no doubt occured, but the extent is undetected by the Mössbauer effect because of the low relative count rate.

Monitoring the gas phase with a mass spectrometer or a thermal conductivity detector would provide an accurate assessment of N_2 loss.

Mössbauer spectroscopy is more successful in observing the bulk transformation in an ε-$Fe_{2.52}N$ sample which is treated at 523 K in 100 ml/min He for 4 hours. Spectral parameters for the beginning and final material's Mössbauer spectra (Figure 12 a and b) are presented in Table 4.3. The isomer shifts and hyperfine fields of the two magnetic species are characteristic of ε-II and ε-III sites. The doublet is attributed to the Fe-Q species. Going from Figure 12a to 12b, the epsilon 2nn and 3nn fields increase by 3-5 kOe. This is indicative of a loss in nitrogen-occupied interstices in the He treated specimen. The nominal stoichiometry of this treated phase is calculated to be $Fe_{2.53}N$, which also suggests an overall N loss. As the peak widths have not broadened in the computer fit to the $Fe_{2.53}N$ spectrum, the distribution of interstitial N throughout the iron matrix is likely to be homogeneous. This implies that nitrogen removal in He is sufficiently slow at 523 K that N rearrangement is possible, and severe interstitial nitrogen gradients are avoided.

Figure 12c gives the Mössbauer spectrum of a single phase γ'-Fe_4N sample, which is subsequently isothermally treated with 100 ml/min He at 523 K for 5 hours (Figure 12d). The Mössbauer parameters describing the three characteristic γ' sites and an Fe-Q species (see Table 3) deviate only slightly for each spectrum. A slight increase in the 2nn: 0nn area ratio occurs in the He treated sample due to a smaller γ'-I area contribution. This is not sufficiently significant to be attributed to a displacement of some two nearest nitrogen into a

Figure 12 Mössbauer Spectra of He Treated Nitrides.

a) ε -$Fe_{2.52}N$

b) ε -$Fe_{2.52}N$ treated in He at 523 K for 4 hours

c) γ'-Fe_4N

d) γ'-Fe_4N treated in He at 523 K for 4 hours

e) γ'-Fe_4N treated in He at 523 K for 1.3 hours then at 598 K for 1.3 hours

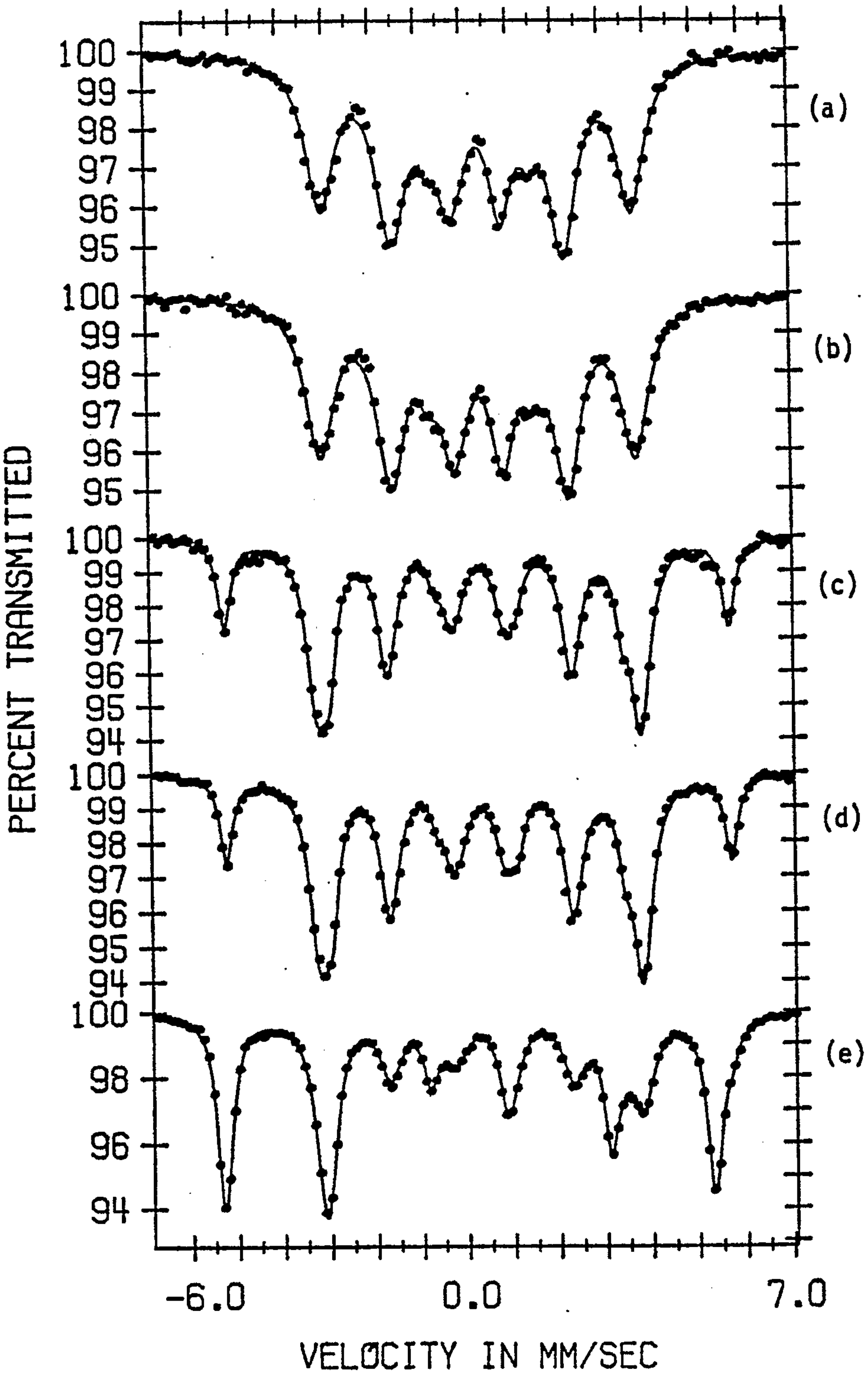
PERCENT TRANSMITTED
100
99
98
97
96
95
94
(a)
(b)
(c)
(d)
(e)
-6.0
0.0
7.0
VELOCITY IN MM/SEC

Figure 12

TABLE 3

Mössbauer Parameters (298 K) of He Treated Nitrides

Figure	Iron Identity	IS (mm/s)	QS (mm/s)	HFS (kOe)	LW (mm/s)	RA (%)	Total Area
12a	ε-II	0.33	0.00	209.0	0.73	61.2	.2858
	ε-III	0.41	0.00	112.4	0.65	30.4	
	Fe-Q	0.32	1.15	---	0.53	8.2	
12b	ε-II	0.32	0.00	212.4	0.73	62.4	.2852
	ε-III	0.40	0.00	117.0	0.62	27.1	
	Fe-Q	0.33	1.13	---	0.54	10.5	
12c	γ'-I	0.23	0.00	339.4	0.33	22.2	.2317
	γ'-IIA	0.29	-0.14	218.1	0.47	49.9	
	γ'-IIB	0.31	+0.34	215.4	0.47	25.0	
	Fe-Q	0.29	1.37	---	0.33	2.9	
12d	γ'-I	0.24	0.00	339.4	0.32	20.3	.2408
	γ'-IIA	0.30	-0.13	217.7	0.49	50.4	
	γ'-IIB	0.31	+0.33	214.6	0.49	25.2	
	Fe-Q	0.33	1.44	---	0.35	4.1	
12e	α-Fe	0.01	-0.01	329.4	0.39	52.3	.2466
	γ'-I	0.22	0.00	338.2	0.56	7.0	
	γ'-II	0.28	+0.04	216.0	0.35	38.8	
	Fe-Q	0.44	1.24	---	0.42	1.9	

previous Onn environment. In fact, one may be mislead into associating a better theoredical envelope fit to the He annealed specimen with a more homogeneous nitride. The lower discrepancy between experimental and predicted values is due to almost twice as many counts in the Figure 12d baseline as in the Figure 8c spectrum.

The final spectrum in Figure 12 clearly shows the effect of γ'-nitride decomposition. A starting γ'-Fe_4N is treated with He at 523 K for 1.5 hours and then at 598 K for an additional 1.5 hours. The spectrum is characterized by superposition of well defined α-Fe and γ'-Fe_4N peaks. The γ' Onn peaks are partially obscured by the stronger Fe^0 contribution, but are apparent in the spectrum: the most negative iron peak (-5.3 mm/s) has greater intensity than the most positive peak (+5.3 mm/s), and the positive side of the latter peak is asymmetric due to the γ' Onn peak at -5.75 mm/s. This overlap is likely to make the 340 kOe difficult to fit accurately. Indeed, for a 39% 2nn contribution, a 13% Onn area is expected. The actual computed γ'-I spectral area is 7%. This spectrum then becomes good illustration of when not to substract component fields. The complexity of computer fitting superimposed contributions can be reduced by combining like fields, as is done with the IIA and IIB sites in this analysis.

The spectral area of α-Fe in Figure 12e is 52%. Ignoring the probable limited solubility of N in the α-iron lattice, the presence of which is indicated by the 0.39 mm/s Fe linewidths being larger than the 0.32 mm/s norm, and (incorrectly) assuming equal recoil-free fractions for Fe and Fe_4N, implies the nitride has lost approximately 50% of its starting nitrogen. Furthermore, as the previous spectra indicated negligible nitride decomposition at 523 K in He, this 50% loss occured during the 1.5 hours of 598 K treatment.

2.3 Transient Kinetics

In our last report (10), we presented Fischer-Tropsch steady state data over each of the nitrides. Most significant was the initial high rate of reaction over all three of the nitrides as compared to α -Fe. This behavior was attributed to the existence of a nitride core, which blocks the competitive carburization of the bulk. In the relatively open bcc lattice of α -Fe, this carburization reaction is so rapid that it inhibits the hydrogenation reactions. After a few minutes of synthesis over the nitrides, however, the activity drops; this is presumably caused by rapid nitrogen loss during this period. Mössbauer spectroscopy has shown that the loss of the nitride phase is extremely rapid during the first few minutes of synthesis. In addition, transient mass spectrometry has revealed the existence of a surface adlayer of a nitrogen containing species that is immediately hydrogenated upon introduction of synthesis gas. Since this nitrogen has been lost, this "opens the door" for carbon to diffuse into the bulk, which causes the competitive carburization reaction to increase and the hydrogenation reaction to decrease. If the first few layers of nitride could somehow be retained, perhaps the initial high activity could also be maintained.

One conceivable way of protecting the bulk nitride is to deposit a carbon overlayer before the catalyst is exposed to hydrogen containing atmospheres. When this pretreated catalyst is exposed to synthesis gas, the bulk is not as readily hydrogenated since nitrogen must now diffuse through the carbon layer. An experiment of this nature was attempted and is shown in Figure 13, in which a freshly prepared nitride was given a one minute pre-exposure to CO at 250°C before exposure to synthesis gas. The ζ-Fe_2N nitride was prepared by flowing pure ammonia over a reduced iron catalyst

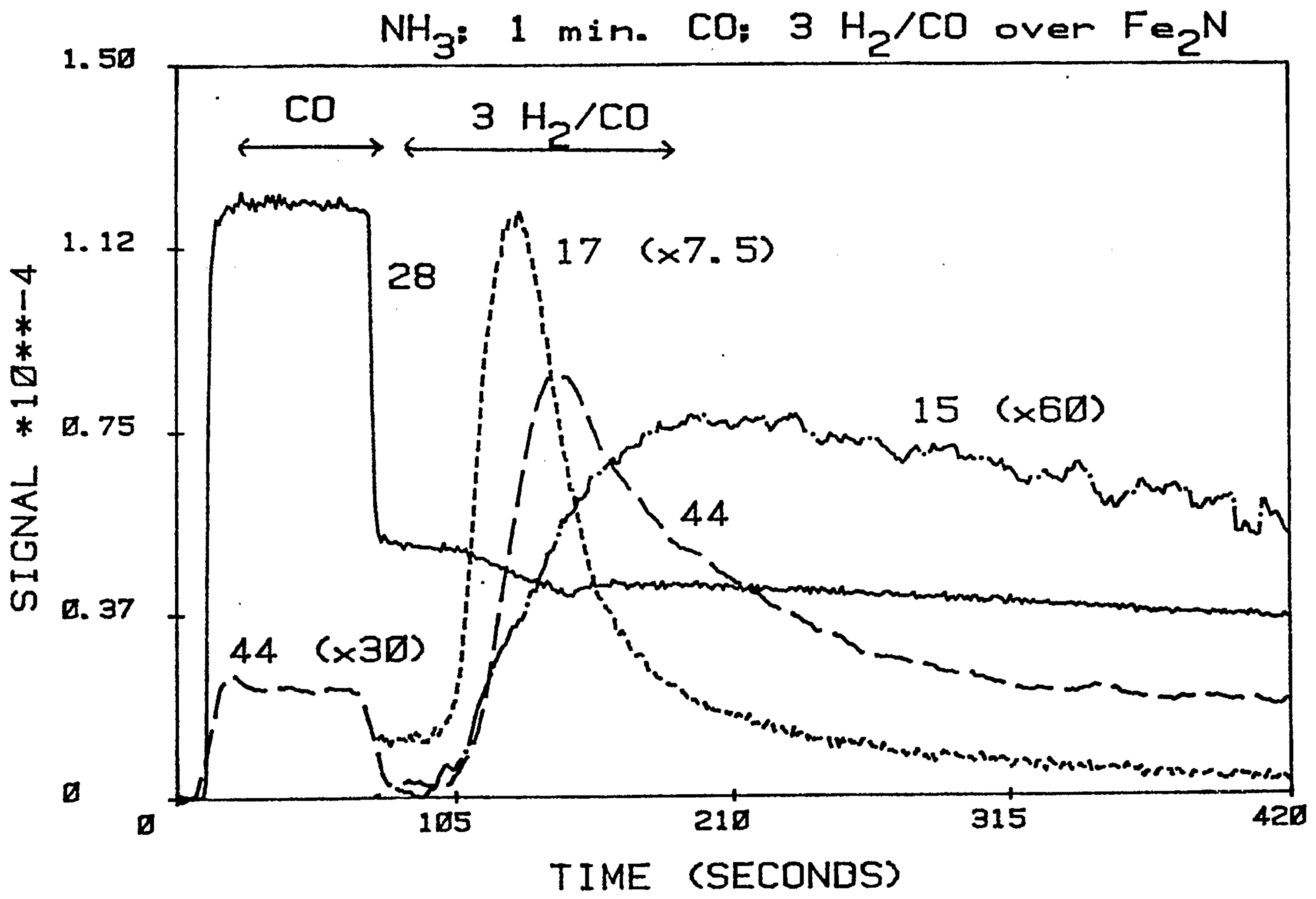

Figure 13 Transient response of Fe_2N to a 1 minute pulse of CO followed by a step to $3H_2/CO$ synthesis gas at 523K. The data are not corrected for fragmentation. Note scale changes.

at 325°C. The temperature was then decreased to 250°C in flowing ammonia.

Figure 13 displays the raw data without calibration to mole fractions or subtraction of contributions due to fragmentations. Pure ammonia (m/e=17), an extremely strong mass spectrometric signal, is off scale at the top of the graph at the extreme left of the Figure. Upon introduction of CO (m/e=28), the ammonia signal drops and a steady state production of CO_2 (m/e=44) occurs. The ammonia signal "tails" since it is only slowly desorbed from the glass wool and tubing walls that make up the reactor system. No other mass signals were observed during the CO treatment.

CO_2 production occurs according to the reaction

$$2\, CO_{ads} \longrightarrow CO_2 + C_{ads}$$

and thus lays down the same amount of carbon as CO_2 produced. Although determination of this amount requires further analysis of this data, it is clear that a fair amount of carbon is deposited in spite of a nearly monolayer coverage of a NH_x species. If carbon deposition blocks sites as well, it is indeed puzzling as to where the CO disproportionation reaction occurs. It would seem that there are insufficient open sites for the steady state CO_2 production observed.

Upon exposure of the CO-Treated catalyst to synthesis gas, no products, other than the continued desorption of NH_3, are observed for the first 20 seconds. If ammonia were being produced from hydrogenation of surface NH_x species during this period, open sites would be formed and the reaction would rise exponentially. The m/e 17 signal does indeed rise exponentially, but only after this 20 second induction period. One could speculate that CH_4 is being produced from the preadsorbed carbon, but at such a slow rate that it is below the sensitivity of the detector. Once enough open sites are available for H_2 adsorption onto active sites (this might be a very small number of open sites), ammonia starts to be produced and the surface is quickly cleared.

On the heels of the m/e 17 peak, CO_2 rises to a later maximum. This phenomenon can be explained by considering the role of CO during the NH_x hydrogenation. As NH_3 is removed, CO is selectively adsorbed from the gas phase. On iron, this species will quickly dissociate. The O_{ads} species can now react with the incoming CO and eventually remove all the surface oxygen, causing the overshoot in CO_2 production. The O_{ads} species does not react with H_{ads}, since this species is selectively producing NH_3. Likewise, the C_{ads} species is not removed as methane (m/e=15) until sufficient ammonia has been removed. Note that the production of methane (m/e=15) and water (m/e=18) is not significant until both ammonia and carbon dioxide have begun to decay.

It would seem that preadsorbed carbon did indeed inhibit the hydrogenation of surface nitride, but only for a brief period. Unfortunately, the preadsorbed carbon inhibited hydrocarbon production as well, and thus rendered the catalyst essentially inactive until it was at least partially removed. Interestingly enough, however, it is seen that the NH_x species did not inhibit the formation of carbon and CO_2 during the CO pretreatment, whereas it is clear that NH_x species need to be removed for significant hydrocarbon production in H_2/CO mixtures.

Other curious phenomenon are also observed in Figure 13 as well. As soon as the gas phase mixture is changed from CO to a H_2/CO mixture, the CO_2 production immediately drops. Since CO is still in the gas phase, and no other significant products are being produced, this must mean that H_2 has replaced the active species for CO_2 production. Paradoxically, this would suggest that the surface now has ample surface hydrogen to catalyze the production of ammonia and other products. Since this is not the case, the sites that produce CO_2 and adsorb hydrogen in CO/H_2 mixtures cannot be active sites for methanation or ammonia production.

Obviously the proposed reaction steps and explanations offered above are complex and need further experimental support before they can be completely accepted. It must be pointed out, however, that Bennett has proposed a dual site mechanism for methane production over iron (11), and Bell has recently observed a large amount of seemingly inactive hydrogen adsorbed on unsupported ruthenium during Fischer-Tropsch synthesis (12). All of these results support theories that the surface is extremely heterogeneous; namely, that adsorption and reaction need not occur on the same type of site.

Further analysis of this experiment and gas chromatograph results of the products formed during the continued FT reaction over this "precarbided" catalyst will be forthcoming. If this pretreatment did indeed partially protect the bulk nitride, the activity would be predicted to be enhanced, according to the competition theory explained above. Similar experiments performed in the Mössbauer should also clarify the effects of CO pretreatment.

3. *Future Research*

Research in the next 3 month period will emphasize the computer fitting of complicated carbonitride peaks in Mossbauer spectra. Transient mass spectral analysis of the decomposition in hydrogen of pre-nitrided catalysts after Fischer-Tropsch synthesis will give additional information on the stoichiometry of the bulk phase during reaction. We will also be working on modelling the denitriding process.

4. *REFERENCES*

1. U.S. Department of Energy Quarterly Technical Progress Report, DOE/PC50804-6
2. Clauser, M.J., Sol. State Comm., *8*, 781 (1970)
3. LeCaër, G., Dubois, J.M. and Senateur, J.P., J. Solid State Chem., *19*, 19 (1976).
4. Chen, G.M., Jaggi, N.K., Butt, J.B., Yeh, E. and Schwartz, L.H., J. Phys. Chem., *87*, 5326 (1983)
5. Jack, K.H., Proc. Roy. Soc. (London)., *A195*, 34 (1948).
6. Bridelle, R., Ann. Chem. Series 12, Number 10, 824 (1955).
7. Anderson, R.B., Cat. Rev.-Sci. Eng., *21*, 53 (1980).
8. Anderson, R.B., Adv. Catal., *5*, 355 (1953)
9. Anderson, R.B., Shultz, J.F., Seligman, B., Hall, W.K. and Storch, H.H., J. Am. Chem. Sco., *72*, 3502 (1950).
10. U.S. Department of Energy Quarterly Technical Progress Report, DOE/PC50804-7
11. Bianchi, D., Tau, L.M., Borcar, S. and Bennett, C.O., J. Catal *84*, 352 (1983).
12. Winslow, P. and Bell, A.T., submitted to J. Cat.

*U. S. GOVERNMENT PRINTING OFFICE: 1985-544-063/10590

Reproduced by NTIS

National Technical Information Service
Springfield, VA 22161

This report was printed specifically for your order from nearly 3 million titles available in our collection.

For economy and efficiency, NTIS does not maintain stock of its vast collection of technical reports. Rather, most documents are custom reproduced for each order. Documents that are not in electronic format are reproduced from master archival copies and are the best possible reproductions available.

Occasionally, older master materials may reproduce portions of documents that are not fully legible. If you have questions concerning this document or any order you have placed with NTIS, please call our Customer Service Department at (703) 605-6050.

About NTIS

NTIS collects scientific, technical, engineering, and related business information – then organizes, maintains, and disseminates that information in a variety of formats – including electronic download, online access, CD-ROM, magnetic tape, diskette, multimedia, microfiche and paper.

The NTIS collection of nearly 3 million titles includes reports describing research conducted or sponsored by federal agencies and their contractors; statistical and business information; U.S. military publications; multimedia training products; computer software and electronic databases developed by federal agencies; and technical reports prepared by research organizations worldwide.

For more information about NTIS, visit our Web site at http://www.ntis.gov.

NTIS

Ensuring Permanent, Easy Access to U.S. Government Information Assets

SATISFACTION GUARANTEED

NTIS strives to provide quality products, reliable service, and fast delivery. Please contact us for a replacement within 30 days if the item you receive is defective or if we have made an error in filling your order.

► E-mail: info@ntis.gov
► Phone: 1-888-584-8332 or (703)605-6050

U.S. DEPARTMENT OF COMMERCE
Technology Administration
National Technical Information Service
Springfield, VA 22161   (703) 605-6000